Macromolecules
ARTICLE

Macromolecules **2009**, *42*, 8875–8881 **8875**
DOI: 10.1021/ma901617u

Polymer Dynamics of Well-Defined, Chain-End-Functionalized Polystyrenes by Dielectric Spectroscopy

Reidar Lund,*[†] Sandra Plaza-García,[†,‡] Angel Alegría,[‡,§] Juan Colmenero,[†,‡,§] Jonathan Janoski,[⊥] Sumana Roy Chowdhury,[⊥] and Roderic P. Quirk[⊥]

[†]*Donostia International Physics Center, Paseo Manuel de Lardizabal 4, 20018 San Sebastián, Spain,* [‡]*Centro de Física de Materiales (CSIC-UPV/EHU), Materials Physics Center (MPC), Apartado 1072, 20080 San Sebastián, Spain,* [§]*Departamento de Física de Materiales, Universidad del País Vasco (UPV/EHU), Paseo Manuel de Lardizabal 4, 20018 San Sebastián, Spain, and* [⊥]*Institute of Polymer Science and Polymer Engineering, The University of Akron, Akron, Ohio 44325-3909*

Received July 22, 2009; Revised Manuscript Received October 16, 2009

ABSTRACT: A novel strategy is described to study polymer dynamics by using a combination of dielectric spectroscopy and functionalized polymers. The first results are presented using various well-defined, chain-end-functionalized polystyrenes (PS) synthesized using a combination of modern anionic polymerization techniques and hydrosilylation chemistry. The end-functionalized polystyrenes investigated contain the cyano (−CN), hydroxyl (−OH), acetyl ($-OCOCH_3$, −Ac), or ethyl ether ($-OCH_2CH_3$, −OEt) groups. By applying broadband dielectric spectroscopy (BDS) over an extensive temperature range (approximately 50−413 K), it was possible to fully characterize the polymer dynamics associated with the segmental α-relaxation as well as the local secondary process related to the specific movement of the functional groups themselves. Combining these data with the results from differential scanning calorimetry (DSC), it is shown that for rather large functional groups the overall polymer matrix properties are altered, giving rise to a decrease in the glass transition temperature. The trend can be rationalized in terms of free volume effects caused by the bulky functional groups and points toward matrix plasticization effects. However, for cyano-functionalized PS the inclusion of this group does not significantly affect the matrix properties. By taking advantage of the strong dipole moment of the CN group, a clear dielectric signal can be obtained that can be used to selectively study the specific dynamics where the group is located. In other words, by appropriately attaching cyano groups at different parts of the chains, these can be exploited as in situ dielectric probes that allow determination of specific contributions to dynamical processes in polymers.

Introduction

Functionalized polymers typically consist of regular polymers with specific chemical groups attached to the backbone, e.g., specific groups in the main chain (in-chain functionalized) or at the end of the chain (chain-end functionalized). From a practical point of view, such systems are very interesting because inclusion of chemical groups via modern synthetic techniques may offer a facile way of modifying and tuning the physical/chemical properties of polymers.[1] This can, in turn, be interesting for application purposes where such polymers may prove useful, e.g., as compatibilizers in composite or filler materials or to alter specific surface properties and/or facilitate specific chemical reactions. However, to fully exploit the potential of these materials, general effects of functionalization on the overall polymer properties have to be understood.

From a more fundamental point of view, well-defined, functionalized polymers in combination with broadband dielectric spectroscopy (BDS)[2] may offer an elegant way to study polymer dynamics because by inclusion of polar groups the dipole moment can be selectively altered. In this way, by selectively amplifying the dielectric signal, it was envisioned that it might be possible to determine relationships and correlations of individual fluctuations contributing to the overall chain dynamics by "labeling" a polymer with covalently bound, polar groups in well-defined positions along the chain. Such an approach offers clear advantages over classical experiments usually involving mixing small molecules as probes into a polymer matrix and measuring the effective local response by some means.[3−5] First of all, the latter approach provides a less direct way of evaluating the polymer dynamics simply because the probe is not necessarily directly "slaved" to the chain dynamics. Second, as the second probe molecule often is of very different nature from the polymer matrix, the mixing may result in significant thermodynamic perturbations that may change or interfere with the dynamics of the polymer,[6] leading to plasticization effects[5] or even phase separation.[7] However, on the other hand, the required polymer functionalization is not trivial: First, it requires control of the polymer synthesis such that the functional groups are located at well-defined and predetermined places in the chain. Second, the appropriateness of the polar group as a selective but "soft" probe must be evaluated; thus, other effects of the polar group, such as changes in the overall polymer matrix properties, must be carefully evaluated and, if necessary, deconvoluted. This requires a combination of techniques using, for example, rheology or calorimetry that are sensitive to the overall matrix properties coupled with BDS that is more sensitive to the polar groups.

Herein, we present the first results from a systematic study of the dynamics of a series of chain-end-functionalized polystyrenes (PS) with a wide range of functional groups. This system is ideal for this purpose because of the low inherent dielectric relaxation signal from the PS backbone. Thus, any signal from the

---

*To whom correspondence should be addressed. E-mail: reidar_lund@ehu.es.

functional groups having much higher dipole moments will be clearly discernible from the unfunctionalized reference analogue. The end-functionalized polystyrenes investigated contain the cyano (−CN), hydroxyl (−OH), acetate (−OCOCH$_3$, −Ac), or ethyl ether (−OCH$_2$CH$_3$, −OEt) groups. The nonfunctional reference is the analogous polymer with an −H group at the chain end. The results show that the cyano group acts like an ideal dielectric probe that does not affect the overall dynamics and can be used to selectively study polymer dynamics.

Experimental Section

Anionic Synthesis of Chain-End-Functionalized Polystyrenes. All preparations of poly(styryl)lithium (PSLi) (M_n = 2200 Da; M_w/M_n = 1.05) were effected in benzene at 30 °C using *sec*-butyllithium as initiator in all-glass, sealed reactors with break-seals and standard high-vacuum techniques as described previously.[8,9] Preparation of the ω-silyl hydride-functionalized polystyrenes was effected directly in the PSLi polymerization reactors by smashing the break-seal for the ampule containing purified chlorodimethylsilane (1.3-fold excess) in benzene at room temperature.[8,9] For the preparation of the ω-functionalized polystyrenes, a 2.5 molar excess of the substituted alkene [e.g., allyl cyanide (Aldrich, 98%) to prepare the ω-cyano-functionalized polystyrene][9] was added to a toluene solution of the ω-silyl hydride-functionalized polystyrene, followed by addition of 0.10 mL of Karstedt's catalyst, 1,3-divinyltetramethyldisiloxane−platinum in xylene (Gelest), as described previously.[8,9] These hydrosilylation reactions were monitored by thin-layer chromatography and FTIR analysis. The residual catalyst was removed from the functionalized polymer by extracting with deionized water, stirring the reaction mixture with activated silica gel, and silica gel column chromatography, followed by treatment with QuadraPure TU, an effective scavenger for platinum.[10] For the preparation of the other ω-functionalized polystyrenes, the corresponding substituted alkenes [allyl alcohol (Aldrich, 99%, dried over 4 Å molecular sieves), allyl acetate (Aldrich, 99%), and allyl ethyl ether (Aldrich, 95%)] were dried over freshly crushed calcium hydride and distilled on the vacuum line into ampules with a Rotoflo stopcock followed by heat-sealing with a hand torch. The reference ω-propyl-functionalized polystyrene was prepared by charging a miniclave containing the ω-silyl hydride-functionalized polystyrene, toluene, and Karstedt's catalyst with 100 psi of propylene (Advanced Gas Technologies, 99.5%) at room temperature for 5 days.

Broadband Dielectric Spectroscopy (BDS). The complex dielectric permittivity vs frequency was measured in the frequency range between 10^{-2} and 10^7 Hz using a Novocontrol high-resolution dielectric analyzer (Alpha-S analyzer). The polystyrene-based samples are brittle solids at room temperature and were prepared directly on two gold-plated electrodes with diameters of 20 and 30 mm, respectively, by heating and drying at 130 °C for 24 h. Subsequently, while hot, the samples were squeezed between the plates using a finely cut 0.1 mm thick, star-shaped Teflon piece as spacer. Finally, before being inserted into the instrument, the samples were briefly placed under vacuum for some minutes at 130 °C to remove any trapped air bubbles, etc. The standard setup consisted of a Novocontrol Quatro cryostat with N$_2$ jet gas which was used in the temperature range of 110−413 K where a stability better than ±0.2 K was achieved. For the low-temperature measurements, a Clod head closed cycle He-refrigerator cryostat from CTI-Cryogenics was used. This provides an accessible temperature range from about 10 to 320 K and a stability of ≈0.2 K.

Differential Scanning Calorimetry (DSC). The calorimetric measurements were carried out using a Q2000 TMDSC from TA Instruments. The sample mass for these measurements was about 8−10 mg. Samples were encapsulated in standard hermetic aluminum pans, and a gas flow (He) was used for thermalization. Corrections for asymmetry relative to reference pan, difference in aluminum pan weight, etc., were performed using the standard procedure of online correction for the DSC Q2000 ("TzeroTM method"). The experiments were carried out by first letting the sample equilibrate at 120 °C and then cooling (20 K/min) to 253 K; thereafter, a temperature modulation of ±0.5 K with a period of 60 s was superimposed on a constant heating ramp of 2 K/min.

Scheme 1. General Methodology for Chain-End Functionalization, Using Anionic Chlorosilane Functionalization Followed by Hydrosilylation

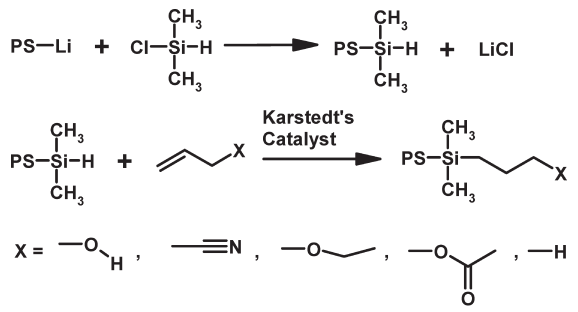

Results and Discussion

Synthesis. For the study of the effects of functional groups on chain dynamics, a new synthetic methodology is available to prepare functionalized polymers in which the only variable between the different polymers is the functional group; all other structural variables are constant.[8,9] This method combines the outstanding structural control of living, alkyllithium-initiated anionic polymerization[11] with the versatility and efficiency of transition metal-catalyzed hydrosilylation reactions.[12,13] This new two-step functionalization methodology is based on anionic synthesis of silyl hydride-functionalized polymers via chlorosilane linking chemistry and hydrosilylation of allyl derivatives (functionalized alkenes) with the silyl hydride-functionalized polymers in the presence of Karstedt′s catalyst, as shown in Scheme 1. All functional polymers were prepared from the same silyl hydride precursor, allowing unparalleled uniformity of polymer chain architecture. In this synthetic procedure, the silyl hydride-functionalized polymer [PS−Si(CH$_3$)$_2$H] provides a versatile platform for conversion to a wide variety of different chain-end-functionalized polymers, designated by PS−Si(CH$_3$)$_2$(CH$_2$)$_3$−X or simply P−X where X denotes the functional group, via hydrosilylation using the corresponding allyl derivatives, CH$_2$=CHCH$_2$−X. For each system, the only variable is the terminal functional end group (−X), since the other end consists of a *sec*-butyl group from the initiator; the molecular weight of the polymer (M_n) and the molecular weight distribution (M_w/M_n) are constant. The molecular weight (M_n) chosen was 2200 Da. Karstedt's catalyst (ppm) used in the hydrosilylation reaction was carefully removed by extraction of the hydrocarbon reaction solution with water, filtration through an activated silica gel column, and treatment for 24 h with QuadraPure TU, which is an effective scavenger of platinum.[10] All chain-end-functionalized polymers were prepared from the same batch of silyl hydride-functionalized polymer and were characterized by FTIR, ^{13}C and ^{1}H NMR spectroscopy, and MALDI-TOF mass spectrometry.[8,9]

Segmental α-Relaxation and the Glass Transition. The dielectric relaxation spectra of the various functionalized polystyrenes are shown in Figure 1. In Figure 1a data obtained at 363 K are shown where the typical α-relaxation associated with the segmental dynamics of the polymers is observed. There are significant differences between the functionalized polymers. This is even clearer in Figure 1b, where data at 343 K, which is closer to the glass transition, are shown. First, as expected, we see that the dielectric signal increases significantly with the inclusion of polar groups. For the cyano functional group, having the largest dipole, the dielectric signal is about a factor of 10 higher than the corresponding reference polymer, P−H. In order to characterize this behavior, we have evaluated the dielectric strength and its relative derivative at T_g, i.e., $\Delta\varepsilon(T = T_g)$ and $1/\Delta\varepsilon(T_g)(\mathrm{d}\Delta\varepsilon/\mathrm{d}T)$. These were obtained by analyzing the real part of the permittivity at low and high frequencies, respectively, and describing the resulting temperature dependence in the high-temperature range ($\approx T_g + 10$ K − $T_g + 50$ K) by a linear law. The results, given in Table 1, show that a similar temperature dependence reflecting the same underlying polymer dynamics, but showing very different $\Delta\varepsilon$, which is expected from the dipole moment strengths. Second, now considering the shape of the spectra, it is seen that the prominent feature of the relaxation of chain-end-functionalized polystyrenes is a significant broadening, generally toward the high-frequency range. This could suggest that the dynamics is more heterogeneous and faster relative to the reference response from P−H. However, for the P−OH sample some indications are seen that the broadening also extends toward low frequencies, suggesting the occurrence of slower components to the dynamics. This might indicate some kind of association perhaps induced by hydrogen bonds between the terminal −OH groups. The influence of interacting functional groups will be the subject of future work where we also plan to apply complementary techniques such as rheology and/or scattering techniques to probe the dynamics. At this point, focus is more on the overall dielectric/dynamical behavior of this series of chain-end-functionalized polystyrenes.

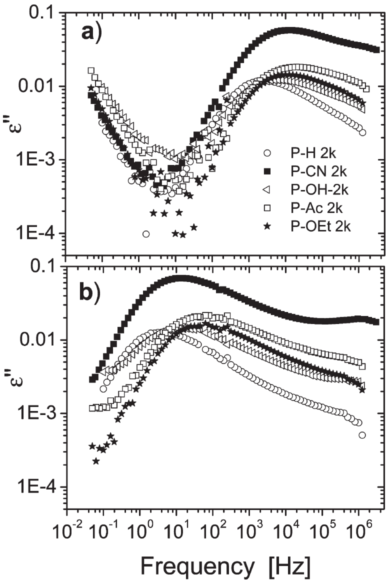

Figure 1. Dielectric loss permittivity, ε'', as a function of frequency for all functionalized polymers showing the typical α-relaxation at (a) 363 K and (b) 343 K.

Extracting a typical relaxation time corresponding to the peak maximum of the dielectric spectra ($\tau^* = (2\pi f^*)^{-1}$, where f^* is the frequency at the peak maximum) as a function of temperature, we see the same general behavior in Figure 2 for all of the chain-end-functionalized polymers. The temperature dependence can be described in the usual way using the well-known Vogel−Fulcher−Tamman phenomenological equation:

$$\tau = \tau_0{}^{\alpha} \exp(B/(T - T_0)) \tag{1}$$

where $\tau_0{}^{\alpha}$ is the elementary time, B, a numerical constant, and T_0 is the so-called Vogel temperature. The parameters obtained from the best fits are given in Table 1.

As seen in Figure 2, while the general trend suggests that all τ^* are generally smaller in the functionalized polymers, there are some peculiarities. Comparing P−CN with P−H at high temperatures, the data seem to be well separated; but when the temperature is gradually lowered, the lines seem to approach each other. To understand this behavior, we have to consider mainly two things: (1) specific dynamics of the chain end where the functional group is located and (2) "self-plasticization" effects induced by the extra free volume created by the chain-end functional groups. For the former it is clear that since with increasing temperature the measurements will be increasingly sensitive to the terminal end-group fluctuations as this dynamics increasingly decouples from the cooperative α-relaxation dynamics. This is due to a decrease of the cooperativity length at high temperatures.[14] Thus, as the temperature is increased, the measured dynamics will more and more reflect the faster end-chain dynamics which will be stronger in dielectric strength the larger the dipole moment of the functional group. Thus, it is clear that at least

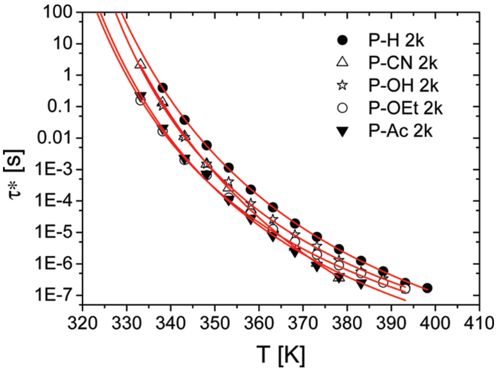

Figure 2. Typical relaxation time corresponding to the peak maximum, τ^*, of the α-relaxation as a function of temperature for all polymers.

Table 1. Parameters of the VFT Fits to the Temperature Dependence of the α-Relaxation Together with the Values for the T_g Deduced from TM-DSC Measurements[a]

polymer	τ_0 [s]	B [K]	T_0 [K]	$T_g{}^D$ [K][b]	T_g [K][c]	$\Delta\varepsilon(T_g)$	d ln $\Delta\varepsilon(T_g)$/dT
P−H	7.10×10^{-14}	1735.8	279.0	334.6	334	0.0744	-1.546×10^{-2}
P-CN	7.00×10^{-14}	1430.9	287.4	334.3	334	0.498	-1.990×10^{-2}
P−OH	1.00×10^{-12}	1277.2	287.8	332.2	331	0.0884	-1.640×10^{-2}
P−OEt	1.00×10^{-12}	1296.4	283.0	327.2	327	0.0955	-1.654×10^{-2}
P−Ac	1.60×10^{-13}	1451.8	281.4	329.4	330	0.130 86	-1.811×10^{-2}

[a] In addition, typical values of the dielectric strength $\Delta\varepsilon$ and its derivative at T_g ($1/\Delta\varepsilon(T_g)(\mathrm{d}\Delta\varepsilon/\mathrm{d}T = \mathrm{d}\ln\Delta\varepsilon(T_g)/\mathrm{d}T)$) are given. [b] Defined according to the temperature where the typical α-relaxation time takes a value of $\tau^* = 10$ s. [c] Calorimetric glass transition temperature defined as the maximum of the derivative of C_p ($\mathrm{d}C_p/\mathrm{d}T$).

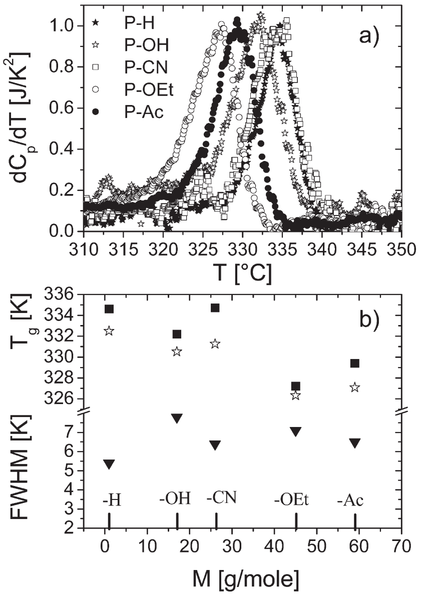

Figure 3. (a) Derivative of the heat capacity, dC_p/dT, as a function of temperature for the various polymers. For clarity only every 10th point is shown. (b) Glass transition temperatures, T_g, determined from calorimetry (filled squares) and T_{gD} determined from dielectric spectroscopy (open stars). The latter values have been determined by defining T_{gD} as the point where the typical relaxation time, τ^*, takes a value of 10 s. Also shown is the full width at half-maximum, fwhm, values (filled triangles) deduced from the data in (a).

a portion of the observed accelerated and heterogeneous dynamics may be attributed to the dominant contributions of these end segments. However, to extract the specific chain dynamics, it is necessary to deconvolute the two effects.

In order to detect potential modifications in the overall matrix properties as distinct from specific chain dynamics, the glass transition, T_g, was also measured using temperature-modulated, differential scanning calorimetry (TM-DSC). The reversing heat flow data exhibit typical behavior for amorphous polymers without specific features apart from a well-defined jump in the specific heat capacity associated with the glass transition of the polymer. In Figure 3a, the derivative of the heat capacity, dC_p/dT, as a function of temperature is shown. In this presentation, the glass transition temperature can be easily identified as the peak temperature. In addition, the width of the transition can be characterized by defining the full width at half-maximum (fwhm) value of the peaks. The values for T_g, extracted both from BDS and DSC, are plotted with the fwhm values as a function of the molar mass of the functional group in Figure 3b.

As seen, the data clearly show that while for the cyano-functionalized polymer T_g remains essentially identical to the reference P−H polymer, the value systematically decreases for the other groups. Interestingly, the values seem to decrease with increasing "bulkiness" or volume of the functional group. Thus, for the P−OEt and P−Ac, T_g corresponds to about 330 and 327 K, respectively, which represents a significant reduction from the value of 334 K of the reference polymer. Now, focusing on the values for fwhm, the values seem to stay roughly constant in most cases, although for P−OH there is a significant increase. This is consistent with the relatively broader low-frequency dielectric response found previously. Also in the other cases, the functionalized polymers display a slightly larger fwhm than the unfunctionalized reference P−H. Hence, these findings and the variation of the T_g values suggest that there are some alterations in the matrix properties caused by the introduction of the functional group. However, it is clear that the alteration is minimal when the group is rather small, e.g., CN, and that it increases in magnitude with the size of the group. It is useful to compare these calorimetric values with the so-called dielectric glass transition temperature, T_{gD}, here defined as the temperature where the typical α-relaxation time corresponds to a fixed value of 10 s ($\tau \equiv 10$ s). As seen in Figure 3b, the data show a trend comparable to the calorimetric data. Interestingly, this is also the case for the cyano-functionalized polymer which displays almost the same T_g as the reference P−H polymer despite the fact that the dielectric spectra have very different shapes. This issue will be discussed again later in the paper. To understand the T_g reduction, one can consider free volume effects associated with the terminal segments including the functional group. The larger the functional group, the more free volume would be created. This can be considered as a sort of an internal or self-plasticization effect where the extra mobility is not created by a separate molecule, as in typical plasticized polymer matrices, but by the bulky functional group itself.

Summarizing the results so far, it can be seen that the bulky end groups may affect the overall dynamics of the polymer matrix by acting as a sort of plasticizer. This gives, in general, accelerated and broader (more heterogeneous) dynamics. For the P−OH polymers, indications of slower dynamic components are observed; it is tentatively suggested that this results from the formation of hydrogen bonds that are much stronger than normal van der Waals forces. For small, noninteracting functional groups such as CN, however, no significant changes are observed in the overall dynamics compared to the reference compound as deduced from the calorimetric T_g.

This was also verified using rheology where the same melt viscosity was observed as well as the same storage and loss modulus for the two references and two cyano-functionalized polymers (M_n = 2200 and 4000 Da) was observed.[15] Hence, with this system it is possible to investigate the specific contributions of functional groups to the overall chain dynamics using dielectric spectroscopy, which inevitably will be most sensitive to the fluctuations of the strong polar groups located at the chain ends. Thus, we can then extract the "pure" chain-end fluctuation dynamics from the overall dynamics by directly subtracting the BDS spectra of the nonfunctionalized reference polymer from the P−CN response. This is done in Figure 4a where the typical raw data (P−CN and P−H) and the subtracted data (−CN) are shown at a representative temperature of 353 K. As clearly seen from this plot, the dynamics of the end-chain cyano groups dominate the P−CN signal. Hence, in this way one can directly observe the fluctuations from the chain ends, which was found to be faster and more heterogeneous than the main-chain (average) response. This shows that in a polymer chain the contributions from the chain end lead to a larger degree of heterogeneity, which thus explains a change in the width of the α-relaxation with decreasing molecular weight.[16] It is also clear that there is a high-frequency wing for the P−CN samples. This comes from an extra winglike contribution that cannot be resolved as a peak at lower temperatures, which is clearly associated with the end-group motion.

Figure 4b shows the typical relaxation time of the α-process of the reference polymer and the contribution from the cyano chain-end fluctuations—the latter data obtained from the subtraction of the spectra. Interestingly we see that, at high temperature, where the dynamics is not expected to be very cooperative, the motion of the end segments with the

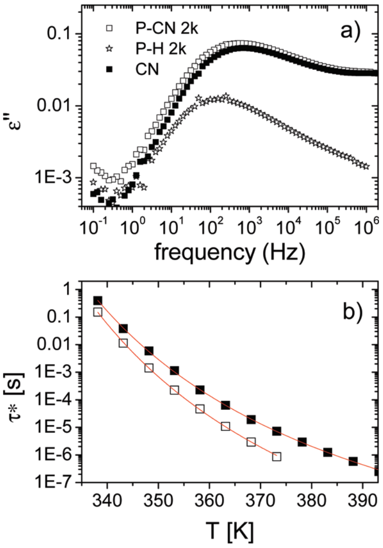

Figure 4. (a) Comparison of the dielectric spectra of P$-$H and P$-$CN and the subtracted spectrum (CN), which corresponds to the specific signal of end-chain fluctuations, e.g., the fluctuations of the segments connected to the cyano group. The latter spectrum was obtained by direct subtraction of the P$-$H from the P$-$CN signal. (b) Corresponding temperature dependence of the typical relaxation time, τ^*, of the overall dynamics (filled symbols) and that of the cyano end-chain dynamics (open symbols).

cyanide group are considerably faster than the average dynamics. However, at progressively lower temperatures, the two time scales seem to merge toward a common glass transition temperature. This important result can be interpreted in terms of a growing cooperativity length into regions named cooperative rearranging regions (CRR) upon a decrease in temperature in line with ideas presented by Adam and Gibbs.[14] The idea is that at low temperatures the dynamics reflect an average over many types of segments, including end-chain segments, since the cooperativity length is large. This cooperativity length gradually decreases with increasing temperature, and the motion gradually reflects single segment motion. Within the Adam$-$Gibbs-type models, studies have shown that this is typically on the order of 1$-$3 nm depending on the temperature[17,18] around the glass transition. While such length scales cannot be extracted from the data in the current study, it can be seen that the results are at least compatible with such a view. It should be noted that the size corresponding to the molecular volume of the end group must be the lower limit to the CRR; i.e., the size of the CRR must be larger than the size of the end group, which can be roughly estimated to be on the order of 0.5 nm. Thus, only at temperatures corresponding to CRR smaller than 0.5 nm independent motion can be expected.

Local Secondary Relaxations Associated with the Functional Groups. The dielectric response at the very lowest temperatures can provide insight into the local secondary relaxations associated with the functional groups. Typical dielectric loss spectra are shown in Figure 5a for all polymers at 110 K. More data over the extended temperature range 110$-$145 K are given in the Supporting Information. Here, a clear relaxation process is visible as a rather broad peak for all functionalized polymers, which is not present in the P$-$H nonfunctionalized reference polymer (see the filled circles in Figure 5a). The signal increases with the strength of the dipole moment of the functional group. Thus, this relaxation process is likely associated with the specific movement of the rather flexible chain-end segment containing the functionalized group inside the frozen glassy polymer matrix.

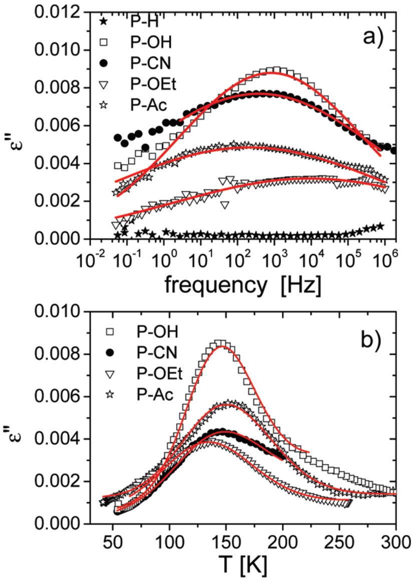

Figure 5. Comparison of the shape and width of the secondary relaxation of the various functionalized polymers: (a) isothermal measurements where ε'' is plotted as a function of frequency at 110 K; (b) isochronal measurements of ε'' as a function of frequency at $f = 1 \times 10^5$ Hz. For clarity, only every second data point is shown.

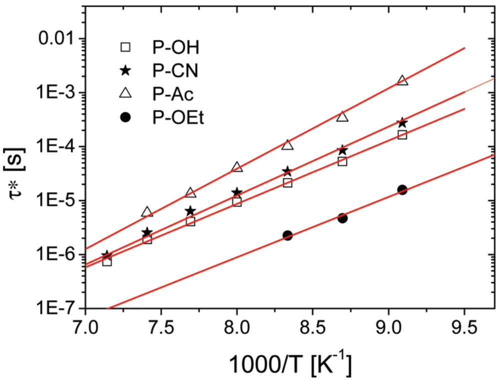

Figure 6. Temperature dependence of the secondary process. Here the logarithm of the characteristic time is plotted versus the inverse temperature in a so-called Arrhenius representation. Note that the data for P$-$OEt are deduced from the data from the isochronal measurements.

In a straightforward manner, the typical relaxation time can be extracted in terms of the position of the peak maxima, τ^*. This is shown in Figure 6 where the logarithm of τ^* is plotted versus the inverse temperature, $1/T$, in a typical Arrhenius plot. Straight lines are observed, thus indicating a pure activated process, as usually seen for secondary processes, following the well-known Arrhenius equation:

$$\tau^* = \tau_0{}^s \exp(E_a/RT) \tag{2}$$

where $\tau_0{}^s$ is the elementary time, R is the gas constant, and E_a is the activation energy. From this simple correlation, it can be seen that the activation energy seems to be higher for the $-$Ac group than for the $-$CN, $-$OEt, and $-$OH groups, suggesting that E_a increases with the size of the functional group. The prefactor was found to be 2$-$3 orders of magnitude lower than 10^{-13} s, which is typical for activated processes. Here, in addition to the enthalpic term, such a process contains an entropic contribution to the free energy of the activated complex. From the values of 100$-$1000 configurational states, we can estimate a entropic term of the order of 40$-$60 J K^{-1} mol^{-1}, which is reasonable.

In order to obtain more detailed information about this process, the temperature dependence and the relaxation width were also investigated. This was done by modeling the local process as a superposition of individual Debye processes (single relaxation time), where the relaxation time distribution arises from a Gaussian distribution of activation energies as shown in eq 3

$$g(E_a) = \frac{1}{\sqrt{2\pi}\sigma_{E_a}\langle E_a\rangle} \exp\left(-\frac{(E_a - \langle E_a\rangle)^2}{2\sigma_{E_a}{}^2\langle E_a\rangle^2}\right) \qquad (3)$$

where σ_{E_a} is the relative width and $\langle E_a\rangle$ is the mean activation energy. In this approximation both are assumed to be temperature independent. The total contribution to the relaxation can then be written as

$$\varepsilon''_s(\omega) = \Delta\varepsilon(T) \int g(E_a) \frac{\omega\tau(E_a)}{1 + \omega^2\tau(E_a)^2} \, \mathrm{d}E_a \qquad (4)$$

where $\omega = 2\pi f$ and $\Delta\varepsilon(T)$ is the dielectric strength. The latter can be modeled as $\Delta\varepsilon(T) = \Delta\varepsilon_0 + AT$, where A and $\Delta\varepsilon_0$ are numerical coefficients. The results of the fits are given in Figure 5. As seen, this simple model provides a full quantitative description of the data around the loss peak.

Despite the general good fits quality obtained in the case of P−OEt, the local process cannot be entirely resolved in the given temperature range restricted to 110 K. The dynamics here is simply too fast, and lower temperatures are needed to characterize this process. This can be seen in more detail in Figure 5a where all polymers are compared at the lowest temperature (110 K). For this reason, measurements have also been performed down to about 30 K using a specially designed dielectric cell and a helium-based cryostat. Because of the extremely low level of dielectric losses at these temperatures, it proved difficult to accurately analyze the isothermal spectra. Therefore, a set of isochronal experiments was performed where several fixed frequencies were measured and the temperature was continuously varied. The associated dielectric losses in a temperature range of about 30−300 K at a fixed frequency of $f = 1 \times 10^5$ Hz are shown for all samples in Figure 5b.

As seen in Figure 5, both the isochronal and isothermal experiments display very similar results where P−OEt exhibits the fastest dynamics. Considering the widths of the peaks, P−OH displays a narrower response as compared with the peaks for P−CN, P−OEt, and P−Ac. In order to obtain very detailed and consistent information, an analogous analysis was performed for the isochronal spectra using the same model of a Gaussian distribution of activation barriers (eq 4). However, in this case it is necessary to take into account a background contribution, which is also visible in the isochronal spectra of Figure 5. Here, a linear parametrization was chosen, $BG = C_0 + DT$, where C_0 and D are simple numerical constants that would be valid only for a limited temperature range. This allows a consistent description of all considered frequencies simultaneously. As seen in Figure 5b, this description works rather well—in particular at low temperatures. However, at high temperatures the linear parametrization of the background signal clearly breaks down as can be deduced from Figure 6b. Nevertheless, as seen in Figure 5, the main feature of the contribution from the local relaxation is consistently described by the model. In order to extract the most reliable and consistent results, both the isothermal and the isochronal data were fitted iteratively in an alternating fashion until a good description of all data was obtained. The parameters relevant for the dynamics, $\langle E_a\rangle$, σ_{E_a}, and $\tau_0{}^s$, are listed as a function of the molar mass of the end groups in Table 2.

Table 2. Extracted Parameters from the Fits Using a Model Representing a Gaussian Distribution of Single Debye Processes

polymer	$\langle E_a\rangle$ [kJ mol^{-1}]	σ_{E_a}	$\tau_0{}^\beta$ [s]	$\Delta\varepsilon_0$	A [K^{-1}]
P−OH	23.0 ± 0.5	0.22 ± 0.05	2.31×10^{-15}	0.069	0.00×10^0
P-CN	24.5 ± 0.5	0.28 ± 0.03	9.20×10^{-16}	0.0646	2.800×10^{-4}
P−OEt	22.2 ± 1	0.33 ± 0.05	2.40×10^{-16}	0.033	9.00×10^{-5}
PS−Ac	26.7 ± 0.5	0.28 ± 0.04	1.96×10^{-16}	0.06	-4.00×10^{-5}

As seen, there is a clear difference in activation energies for the local relaxation between the functional groups. Although the trend is not smooth and the interpretation is not straightforward, it can be seen that from P−OH to P−Ac the activation energy increases from about 23 to 27 kJ/mol. However, to understand this, several factors must be taken into account. First, on an intuitive basis, the activation energies would be expected to be related to the size, i.e., the volume or mass, of the functional group and to increase with increasing size. This explains the general trend, particularly for P−OEt, which exhibits the lowest value for $\langle E_a\rangle$ and the largest value for σ_{E_a} among the functional groups. Thus, it can be speculated that this reflects a more heterogeneous polymer matrix. It can also be seen that the relative width (Figure 6a) of the local relaxation is significantly smaller for the P−OH (~20%) than for the cyano-functionalized polymer (~30%) which might be expected since the functional group is smaller and thus the group is less sensitive to the free volume. Finally, one must take into account the specific chemical bonds responsible for a movement (rotation, vibration, etc.) that is dielectrically active. After an inspection of the end-group structures in Scheme 1, it is clear that in all cases except one, P−CN, the active bonds are of the C−O bond type, which with an appropriate rotation would yield a significant change in dipole moment. For the P−CN sample, however, a dielectrically active movement can only occur via a C−C bond rotation or an oscillation around the C−C≡N angle. Since the C−C≡N unit is linear, a rotation around this end group is not dielectrically active. This is different from the P−OH in which a simple rotation around the C−OH bond will be dielectrically active and, because of the smaller total mass, will have a smaller $\langle E_a\rangle$. In addition, by further comparing with literature data from spectroscopy, a value of $E_a = 13.72$ kJ/mol is found for rotation of the $CH_3{-}CH_2CN$ bond[19] and a significantly smaller $E_a = 4.47$ kJ/mol for rotation of the $CH_3{-}OH$ bond.[20] Thus, a larger activation barrier would be expected for the P−CN polymer than for P−OH, which is indeed observed. From microwave data in the gas phase, smaller rotation barriers relative to the $CH_3{-}CH_2CN$ bond would be expected for the $CH_3{-}OCH_2CH_3$ and $CH_3{-}O_2CCH_3$ bonds ($E_a = 10.92$ kJ/mol[20] and $E_a = 5.10$ kJ/mol,[21] respectively); however, these comparisons with the experimental data seem to correlate well only for the ether group. Hence, it is clear that other factors such as chain packing and more complex motions contribute to the observed behavior. In fact, comparing the data for $\tau_0{}^s$ in Figure 6b, it can be seen that this prefactor decreases monotonously in relation to the size and "complexity" of the functional group. Since the basic polymer structure is the same, this may indicate a more significant entropic contribution and a larger number of dielectrically active steps involved for larger functional groups. In order to elucidate this issue further, complementary techniques such as NMR may be useful.

Conclusions

This work has shown how sophisticated anionic polymerization techniques coupled with hydrosilylation chemistry can be used to label polymer chains by introducing functional groups selectively at the chain end. Thereby, through changing the local dipole moment of the functional end group and by applying broadband dielectric spectroscopy to this kind of system, a very sensitive, selective tool can be created to investigate the dynamics of polymers. By studying both the general α-relaxation visible above the glass transition temperature (T_g) as well as the functional group-specific secondary relaxation observed well below T_g, detailed insight can be gained into the dynamics in these systems. In particular, by comparing various functionalized polymers, the relative contributions of chain ends, in this case, to the cooperative segmental dynamics as well as the correlations to the local functional groups' dynamics can be made. The results show that this functionalization may have an effect on the overall matrix properties whenever the functional group is rather large, e.g., acetate and ethyl ether groups, etc. This leads to a decrease in the glass transition temperature due to an effect that can be called a self-plasticization effect that arises from the extra free volume created by the fluctuations of the relatively large functional end group. However, for functionalized polymers containing cyano groups, no significant effect of the functional group is observed, and the matrix properties are essentially the same as the reference, which is reflected in identical glass transition temperatures and melt viscosities. Since the relative dielectric signals for these polymers are different, this system can further be exploited to extract detailed information about chain dynamics. The results obtained by direct subtraction of the main α-relaxation response, using the data from the reference P−H polymer, show that the dynamics of the end segments is faster and more heterogeneous than the average dynamics. This study thus shows directly how chain ends increase the heterogeneity of the dynamic response in polymers. Interestingly, the data show a merging toward a common glass transition temperature, suggesting an increasing cooperativity in the dynamics as the systems vitrify. In future work, this will be elaborated in more detail by comparing other functionalized polymers, e.g., in-chain functionalized polymers, and other molecular weights.

Acknowledgment. The University of Akron researchers gratefully acknowledge Repsol YPF for partial support of this research and also FMC, Lithium Division, for providing samples of *sec*-butyllithium. The Basque Country Government (IT-436-07) and the Spanish Ministry of Education and Science (MAT 2007-63681), Consolider (Spanish Ministry of Science), are gratefully acknowledged.

Supporting Information Available: Plots of the dielectric loss permittivity, ε'', as a function of frequency for all functionalized polymers. This material is available free of charge via the Internet at http://pubs.acs.org.

References and Notes

(1) Hawker, G. J.; Wooley, K. L. *Science* **2005**, *309*, 1200.
(2) Kremer, F., Schönhals, A., Eds. *Broadband Dielectric Spectroscopy*; Springer-Verlag: Berlin, 2003.
(3) van den Berg, O.; Sengers, W. G. F.; Jager, W. F.; Picken, S. J.; Wübbenhorst, M. *Macromolecules* **2004**, *37*, 2460.
(4) Maji, S.; Urakawa, O.; Adachi, K. *Polymer* **2007**, *48*, 1343.
(5) van den Berg, O.; Wübbenhorst, M.; Piquen, S. J.; Jager, W. F. *J. Non-Cryst. Solids* **2005**, *351*, 2694.
(6) Cangialosi, D.; Alegria, A.; Colmenero, J. *J. Chem. Phys.* **2007**, *126*, 204904.
(7) Cangialosi, D.; Wübbenhorst, M.; Groenewold, J.; Mendes, E.; Schut, H.; van Veen, A.; Picken, S. J. *Phys. Rev. B* **2004**, *70*, 224213.
(8) Quirk, R. P.; Kim, H.; Polce, M. J.; Wesdemiotis, C. *Macromolecules* **2005**, *38*, 7895.
(9) Quirk, R. P.; Janoski, J.; Chowdhury, S. R.; Wesdemiotis, C.; Dabney, D. E. *Macromolecules* **2009**, *42*, 494.
(10) *Reaxa Quadrapure User Guide*; Reaxa Ltd.: Manchester, UK, 2006 http://www.reaxa.com/documents/reaxa_quarapureuserguide.pdf.
(11) Hsieh, H. L.; Quirk, R. P. *Anionic Polymerization: Principles and Practical Applications*; Marcel-Dekker: New York, 1996.
(12) Marciniec, B. *Comprehensive Handbook on Hydrosilylation*; Pergamon Press: Oxford, 1992
(13) Brook, M. A. *Silicon in Organic, Organometallic, and Polymer Chemistry*; John Wiley & Sons: New York, 2000.
(14) Adam, G.; Gibbs, J. H. *J. Chem. Phys.* **1965**, *43*, 139.
(15) Lund, R.; García-Plaza, S.; Alegría, A.; Colmenero, J.; Janoski, J.; Chowdhury, S. R.; Quirk, R. P. To be submitted for publication, **2009**.
(16) Mattsson, J.; Bergman, R.; Jacobsson, P.; Börjesson, L. *Phys. Rev. Lett.* **2003**, *90*, 75702.
(17) Hempel, E.; Hempel, G.; Hensel, A.; Schick, C.; Donth, E. *J. Chem. Phys.* **2000**, *104*, 2460.
(18) Cangialosi, D.; Alegria, A.; Colmenero, J. *Phys. Rev. E* **2007**, *76*, 11514.
(19) Lin, C. C.; Swalen, J. D. *Rev. Mod. Phys.* **1959**, *31*, 841.
(20) Eliel, E. L.; Wilen, S. H.; Mander, L. N. *Stereochemistry of Organic Compounds*; John Wiley & Sons: New York, 1994; p 628.
(21) Williams, G.; Owen, N. L.; Sheridan, J. *Chem. Commun. (Cambridge, U.K.)* **1968**, 57.